A Zero-Watermarking Algorithm for Medical Images Based on Gabor-DCT

Xiliang Xiao[1], Jing Liu[3], Jingbing Li[1,2(✉)], Yangxiu Fang[1], Cheng Zeng[1], Jiabin Hu[1], and Uzair Aslam Bhatti[4]

[1] School of Information and Communication Engineering, Hainan University, Haikou, Hainan, People's Republic of China
{FangYangxiu,18085208210009}@hainanu.edu.cn
[2] State Key Laboratory of Marine Resource Utilization in the South China Sea, Hainan University, Haikou, Hainan, People's Republic of China
[3] Research Center for Healthcare Data Science, Zhejiang Lab, Hangzhou, Zhejiang, People's Republic of China
liujinglj@zhejianglab.edu.cn
[4] School of Geography (Remote sensing and GIS Lab), Nanjing Normal University, Nanjing, People's Republic of China

Abstract. The development of digital age accelerated the development of digital medical systems, but it also inevitably brings security problems of the transmission and storage of medical images in the network. The wide use of digital watermarking technology in medical images has effectively improved such problems, but the research on the medical image watermarking algorithm is still less and immature. How to improve the invisibility and robustness of watermark information is a difficult problem in the medical image watermarking algorithm. In this paper, a zero watermarking algorithm for medical images based on Gabor-DCT is proposed. The watermark information first encrypted by a Logistic chaotic map and then combined with the medical image feature vector extracted by the Gabor-DCT algorithm to improve the robustness of the watermark information. At last, the watermark is extracted and embedded by zero watermark technology, which improved the invisibility of the watermark information. Experimental results show the proposed algorithm can effectively resist both common attacks and geometric attacks, and has good invisibility and robustness.

Keywords: Gabor · DCT transform · Zero watermark · Chaotic sequence · Robustness

This work was supported in part by the Hainan Provincial Natural Science Foundation of China under Grant 2019RC018 and by the Natural Science Foundation of China under Grant 62063004 and 61762033, in part by the Hainan Provincial Higher Education Research Project under Grant Hnky2019-73, and in part by the Key Research Project of Haikou College of Economics under Grant HJKZ18-01.

J. Cheng et al. (Eds.): CSS 2020, LNCS 12653, pp. 144–156, 2021.
https://doi.org/10.1007/978-3-030-73671-2_14

1 Introduction

The modern medical system has entered the process of digitalization. A large amount of patient information is disseminated and stored on the Internet in the form of text and images, which facilitates the medical system. But it also brings more security risks due to the insecurity of the Internet [11,14]. Patients' information are easily be attacked and destroyed during the transmission of the network, or even stolen, with poor security. The development of digital watermarking technologies [8,17] provides good solutions to such problems. Combining medical images with watermarks, and embedding patients' information in the medical image in the form of watermarks can better protect patients' information, which can greatly improve the safety and stability of medical images spreading on the network [1,10].

The concept of digital watermarking was first formally proposed by Tirkel et al. They added the watermark information to the least significant bit (LSB). The method is simple, and the robustness is poor, especially in terms of resistance to geometric attacks [13]. At present, the research in the field of medical image watermarking is still immature. Generally, the embedding and extraction of watermarking are mainly concentrated in the spatial domain and the transform domain [6]. The spatial domain refers to directly embedding watermark information in medical images, while the transform domain refers to transforming the image, and then embedding the watermark information in the transformed data. Medical images are generally divided into regions of interest (ROI) and regions of non-interest (RONI). [4] R. Eswaraiah and E. Sreenivasa Reddy proposed a medical image watermarking technology that can locate the tampered position and restore the ROI by combining the watermark information and the ROI.And the information is embedded in the boundary area and RONI. Divide the region of interest into blocks, find the mean and variance, and determine the tampered position of the region of interest. Then use the restoration data embedded in RONI to restore the ROI. This algorithm can be very effective. Good positioning restores the ROI area information, but it is performed in the airspace. If it is subjected to geometric attacks, its robustness is poor, as the information embedded in the edge area and RONI will also be destroyed. The transform domain methods include DCT transform, Fourier transform, wavelet transform, etc. [7,15], which have better hiding and robustness for watermark information and are more popular by researchers. Siddharth Singh et al. proposed an NSCT-DCT-SVD medical image watermarking algorithm. The algorithm decomposed the medical image and watermark into six subbands by NSCT, and then performed DCT transformation on any subband, and applied SVD on the coefficients after DCT transformation. Decompose, and finally add the weight of the two singular values to realize the embedding of the watermark [12], which has high invisibility and robustness. Compared with the spatial domain, the watermark embedding in the transform domain is more robust and effective, but whether it is the spatial algorithm in [4] or the transform domain algorithm in [12], they all need to change the pixel value or transform coefficient to realize the embedding of the watermark. This may affect the visual characteristics of the images, which is not

desirable for medical images. The development of zero watermark [5,16] solved this problem very well. It has better robustness and invisibility by finding the feature invariant vector of the image and combining it with the watermark.

Gabor texture features are mostly used in face recognition, expression recognition, fingerprint recognition, image index, etc. [3,9]. Since the Gabor transform can extract texture features, it is also used in the watermarking algorithm. [2] In this paper, a Gabor transform-based watermarking algorithm is proposed. The watermark information is hidden by changing the DGT coefficients to represent the special low frequency. However, this method will affect the visual characteristics of medical images. In the field of medical image watermarking, there is little research on Gabor transform to extract texture features. In this paper, the texture features obtained by Gabor filter in different scales and directions are combined with DCT, which greatly improved the robustness of the watermark image against various common attacks and geometric attacks.

2 Basic Theory

2.1 Gabor Texture Features

Gabor transform is a windowed Fourier transform, which is obtained by Gaussian function and the complex sine function. It is similar to human visual cell response, sensitive to image edge, and has good direction and scale selectivity. Compared with the traditional Fourier transform, Gabor wavelet transform has good time-frequency localization characteristics, and is insensitive to illumination. It can adapt to a certain degree of image rotation and deformation.

By generating a set of self-similar Gabor filters(as shown in Fig. 1), texture features in different scales (frequencies) and different directions can be extracted(as shown in Fig. 2). If the input medical image is $I(x, y)$ and the size is $M \times N$, then its Gabor wavelet transform is as follows:

$$W_{uv}(x, y) = \sum_{x_1}^{d_1} \sum_{y_1}^{d_2} I\left(x - x_1, y - y_1\right) g_{uv}\left(x_1, y_1\right) \tag{1}$$

where $W_{uv}(x, y)$ are the texture feature image after the Gabor wavelet transform, and d_1, d_2 are the template size of Gabor filter, which u represent a certain scale (frequency),and v represent a certain direction. $\mathrm{g}_{uv}(x, y)$ are a group of self similar filters after scale transformation and rotation transformation of the mother wavelet $g(x, y)$.

The expression of mother wavelet is as follows:

$$\mathrm{g}(x, y) = \frac{1}{2\pi\sigma_x\sigma_y} \exp\left(-\frac{1}{2}\left(\frac{x^2}{\sigma_x} + \frac{y^2}{\sigma_y}\right)\right) \exp(2\pi \mathrm{j} w x) \tag{2}$$

Where, σ_x and σ_y are the standard deviation of Gaussian function on two coordinate axes, w are the frequency of complex sine function, and the value of σ_x, σ_y is related to bandwidth and inversely proportional to w.

$$\begin{cases} g_{uv}(x,y) = \alpha^{-u} g\left(x', y'\right), \quad \alpha > 1 \\ x' = \alpha^{-u}(x\cos\theta + y\sin\theta) \\ y' = \alpha^{-u}(-x\sin\theta + y\cos\theta) \end{cases} \tag{3}$$

Where α^{-u} is the scale modulation factor (u, v are integers), $\alpha = \left(\frac{U_h}{U_l}\right)^{-\frac{1}{S-1}}$, $\theta = \frac{v\pi}{K}$, S is the number of scales, K is the number of directions, $u = 0, 1, 2, \ldots, S-1, v = 0, 1, 2, \ldots, K-1, U_h$ is the highest spatial frequency, U_l is the lowest spatial frequency.

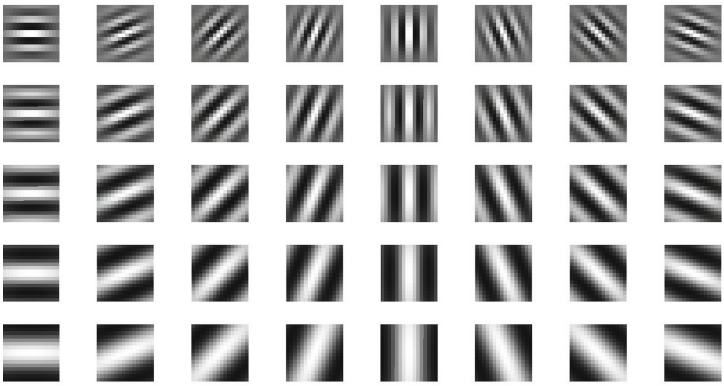

Fig. 1. Gabor filter kernels with different directions and scales

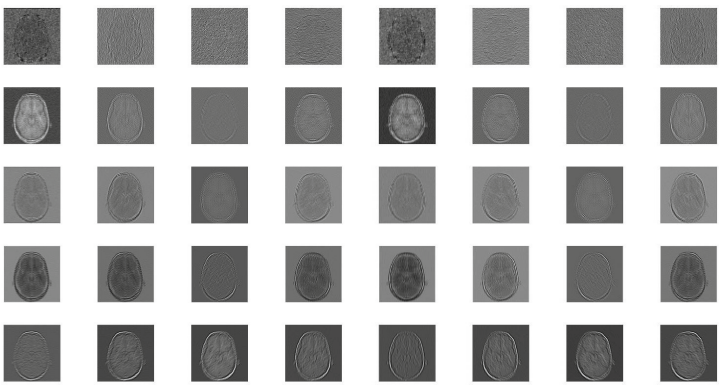

Fig. 2. Texture features of brain images with different directions and scales

The Gabor filter banks are used to extract the texture feature maps of medical images $W_{uv}(x, y)$ in different scales and directions. As the feature dimension is too high, the feature vector G_{uv} (row vector) of each texture feature map is generally obtained by averaging in blocks, and the Eigenvector matrix H (total $S \times K$ row, texture feature vector with one scale and one direction for each row) is constructed:

$$H = \begin{bmatrix} G_{00} \\ G_{10} \\ G_{20} \\ \cdots \\ G_{(S-1)(K-1)} \end{bmatrix} \tag{4}$$

2.2 Discrete Cosine Transform

Since the discrete cosine transform (DCT) was proposed in 1974, it has been loved and recognized by many scholars. It is widely used in image processing, digital signal, and other fields. It is similar to discrete Fourier transform, but only uses the real part. Discrete cosine transform (DCT) can concentrate the data energy in the upper left corner, that is, the low-frequency region, which has the characteristic of "energy concentration". It can realize data compression. Discrete cosine transform is used in standard JPEG, MJPEG and MPEG compression. The expression of 2D-DCT is as follows:

$$F(u, v) = c(u)c(v) \sum_{x=0}^{M-1} \sum_{y=0}^{N-1} f(x, y) \cos \frac{\pi(2x+1)u}{2M} \cos \frac{\pi(2y+1)v}{2\,N} \tag{5}$$

Among them, u = 0, 1, …, M − 1; v = 0, 1, …, N − 1;

$$c(u) = \begin{cases} \sqrt{\frac{1}{M}}, u = 0 \\ \sqrt{\frac{2}{M}}, u = 1, 2, \ldots, M-1 \end{cases} \quad c(v) = \begin{cases} \sqrt{\frac{1}{N}}, & v = 0 \\ \sqrt{\frac{2}{N}}, & v = 1, 2, \ldots, N-1 \end{cases} \tag{6}$$

x, y is the spatial domain sampling value; u, v is the frequency domain sampling value.

2.3 Logistic Map

The logistic map is a kind of nonlinear mapping. Given the initial value and parameters, the chaotic sequence can be obtained:

$$x_{k+1} = \mu \cdot x_k \cdot (1 - x_k) \tag{7}$$

where, μ is the growth parameter and k is the number of iterations, $0 \leq \mu \leq 4, x_k \in (0, 1)$. At that time, $3.5699456 < \mu \leq 4$, the logistic map was chaotic. In this paper, $\mu = 4$, the number of iterations is set $k = 32$.

3 Algorithm Process

Embedding the watermark information into the spatial domain of medical images, once the image is destroyed, the embedded watermark information will be greatly affected, and the watermark restoration effect is generally poor. However, by embedding the watermark information into the feature vector which can represent the image features in the transform domain, zero watermark can be embedded and extracted when the feature vector does not change much when the image is destroyed, so as to improve the invisibility and robustness of the watermark.

3.1 Watermark Encryption

As shown in Fig. 3, firstly, the chaotic sequence is generated by chaotic mapping function. Then binary encryption matrix is obtained by binarization of perceptual hash, and the chaotic encrypted watermark is get by XOR of binary watermark $W(i,j)$ of 32 pixels $\times$ 32 pixels and $C(i,j)$.

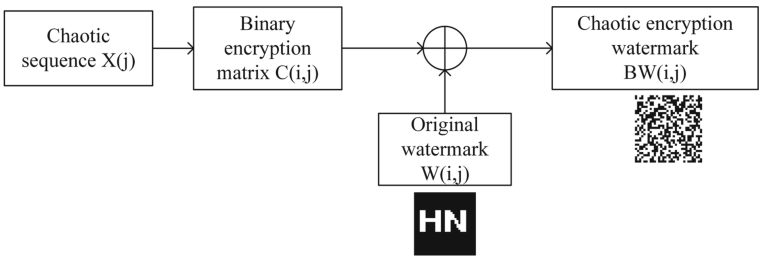

Fig. 3. Watermark encryption process

3.2 Watermark Embedding

For watermark embedding, the original medical image $I(i,j)$ with 512 pixels $\times$ 512 pixels is transformed by Gabor to get the feature matrix $H(i,j)$. And then DCT transform is applied to get the feature vector $V(j)$.The chaotic encryption watermark $BW(i,j)$ and the feature vector are XOR to get the logical secret key $key(i,j)$, which is retained and used in watermark extraction,as shown in Fig. 4.

$$key(i,j) = V(j) \oplus BW(i,j) \tag{8}$$

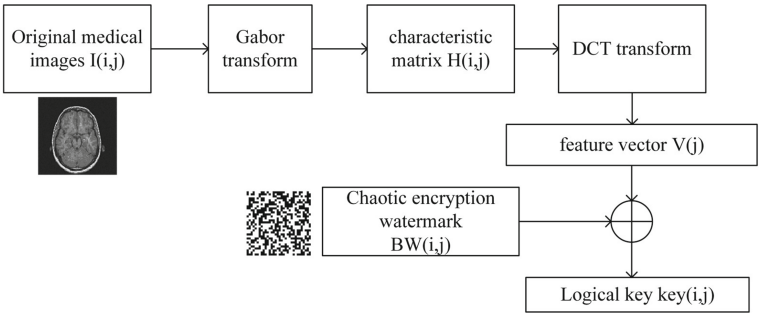

Fig. 4. Watermark embedding process

3.3 Watermark Extraction

As shown in Fig. 5, watermark extraction is the inverse process of watermark embedding. According to the embedding method, the feature vector $V'(j)$ of the image to be tested is extracted, and then XOR processing is performed between $V'(j)$ and the logical secret key $key(i,j)$ to obtain the encrypted watermark $BW'(i,j)$. At the same time, $BW'(i,j)$ do XOR with the binary encryption matrix $C(i,j)$ which was obtained when embedding the watermark to obtain the restored watermark $W'(i,j)$

$$W'(i,j) = C(i,j) \oplus BW'(i,j) \tag{9}$$

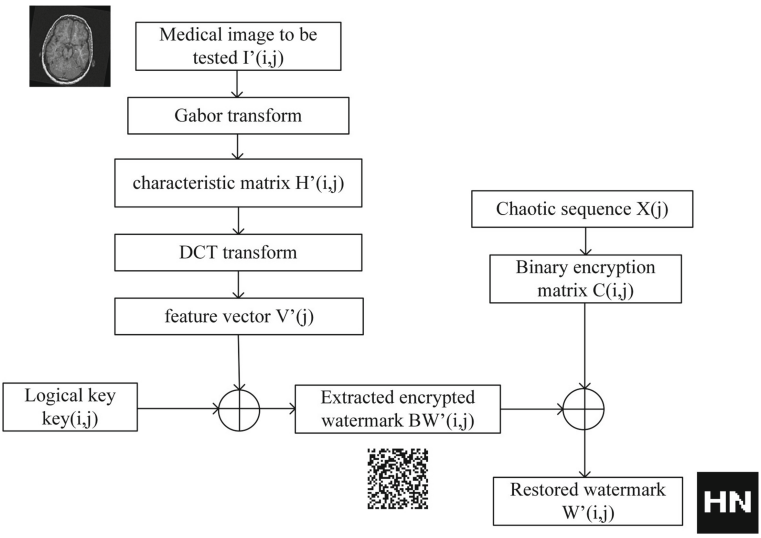

Fig. 5. Watermark extraction

3.4 Performance Metrics

The distortion degree of the medical image can be expressed by the peak signal-to-noise ratio (PSNR/dB), and the restoration degree of the watermark can be expressed by normalized correlation coefficient (NC);

$$PSNR = 10 \log \left[\frac{MNmax_{i,j}(I(i,j))^2}{\sum_i \sum_j \left(I(i,j) - I'(i,j)\right)^2} \right] \tag{10}$$

$$NC = \frac{\sum_i \sum_j W(i,j)W'(i,j)}{\sqrt{\sum_i \sum_j W(i,j)^2}\sqrt{\sum_i \sum_j W'(i,j)^2}} \tag{11}$$

The lower the $PSNR$ value is, the greater the distortion is, and the closer the NC value is to 1 ,the better the watermark restoration is.

4 Experiments and Results

Experiments were performed using Matlab r2015b for all medical images.This paper selects a 512 pixels × 512 pixels medical image brain as the cover image of the watermark. First,a Gabor transformed are performed to obtain feature matrix H, and then do the DCT transformed to the feature matrix H, and the first 32-bit DCT coefficients in the upper left corner are obtained through the Z-scan method. The 32-bit binary sequences obtained by the coefficient sign judgment (the coefficient is positive to be 1, and the coefficient is negative to be 0) is used as the feature vector of the medical images.

As shown in Fig. 6, four different medical images are selected. Table 1 shows the feature vectors extracted from each medical image by Gabor-DCT. It can be seen from the Table 1 that the feature vectors extracted from different medical images are different.

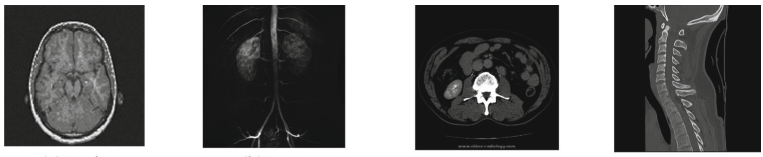

(a)Brain (b)Lung (c)Abdomen (d)Cervical Spine

Fig. 6. Different medical images

Table 1. Feature vectors of different medical images.

Different medical images	Feature sequences
(a) Brain	1100 0011 1000 1010 0001 0001 1010 0110
(b) Lung	1111 1111 1000 1110 1011 0101 0100 1000
(c) Abdomen	1100 0110 1110 1010 0001 0100 1011 1011
(d) Cervical spine	1011 1010 1111 1010 1011 0101 1110 1010

Table 2. PSNR and NC values based on Gabor-DCT under common attacks.

Conventional attack	Gaussian noise			JPEG compression			Median filter (Thirty times)		
	1%	5%	10%	1%	10%	20%	3×3	5×5	7×7
PSNR/dB	20.45	14.31	11.85	26.28	31.29	33.81	33.78	26.92	24.96
NC	0.90	0.80	0.74	1.00	0.90	1.00	1.00	1.00	0.90

4.1 Common Attacks

There are three kinds of common attacks in the experimental: Gaussian noise attacks, JPEG compression attacks and median filtering attacks. Table 2 shows the PSNR and NC values under different attacks intensities.

From Table 2, when the Gaussian noise is 10%, the NC value is 0.74. When the JPEG compression quality is 1%, the NC value is 1.00. For 30 times of 7×7 median filtering, the NC value is still as high as 0.90. At the same time, it can be seen from Fig. 7 that the watermark is still visible after each attacks, that is, the algorithm proposed in this paper can well resist common attacks, especially in the aspect of JPEG compression attacks and median filtering attacks.

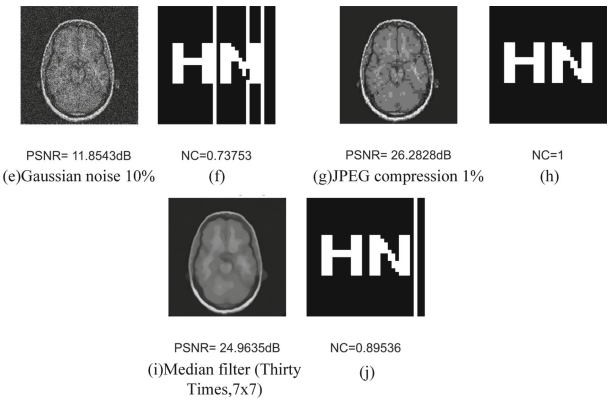

Fig. 7. Medical image after the common attacks and the restored watermark

4.2 Geometric Attacks

Geometric attacks (rotation, scaling, translation, clipping) have a great impact on images. How to improve the robustness of images under geometric attacks have always been a difficult problem. Table 3 shows the test results of the algorithm after several geometric attacks.

Table 3. PSNR and NC values for geometric attacks based on Gabor-DCT.

Geometric attacks	Attack strength	PSNR/dB	NC
Rotation (clockwise)	5°	18.00	1.00
	10°	15.60	1.00
	20°	14.60	0.71
Scaling attack	0.5	/	0.70
	0.8	/	0.90
	2.0	/	0.89
Translation attack (left)	5%	14.48	1.00
	15%	12.86	1.00
	25%	11.42	0.89
Translation attack (right)	5%	14.51	1.00
	15%	12.90	1.00
	25%	11.30	0.81
Crop (Y direction)	5%	/	1.00
	10%	/	0.80
	25%	/	0.61
Crop (X direction)	5%	/	1.00
	15%	/	1.00
	25%	/	0.81

(1) Rotation attacks: When the medical image is rotated 20 degrees, as shown in (k) and (l) in Fig. 8, the PSNR value is very low, but the NC value is 0.71, which still can restore the watermark well, indicating that the algorithm has good robustness against rotation attacks.
(2) Scaling attacks: When the medical image is reduced to 0.5 times, the NC value is 0.71 when the medical image is magnified by 2 times, as shown in (m) and (n) in Fig. 8, the NC value is 0.89 , and the watermark restoration degree is high. It shows that the algorithm is robust to scaling attacks.
(3) Translation attacks: When the left shift and right shift of medical images are all 25%, the NC values are above 0.80. As shown in (o), (p), (q) and (r) in Fig. 8, they are 25% left shift, 25% right shift and corresponding restored watermark. Therefore, the algorithm is robust to translation attacks.

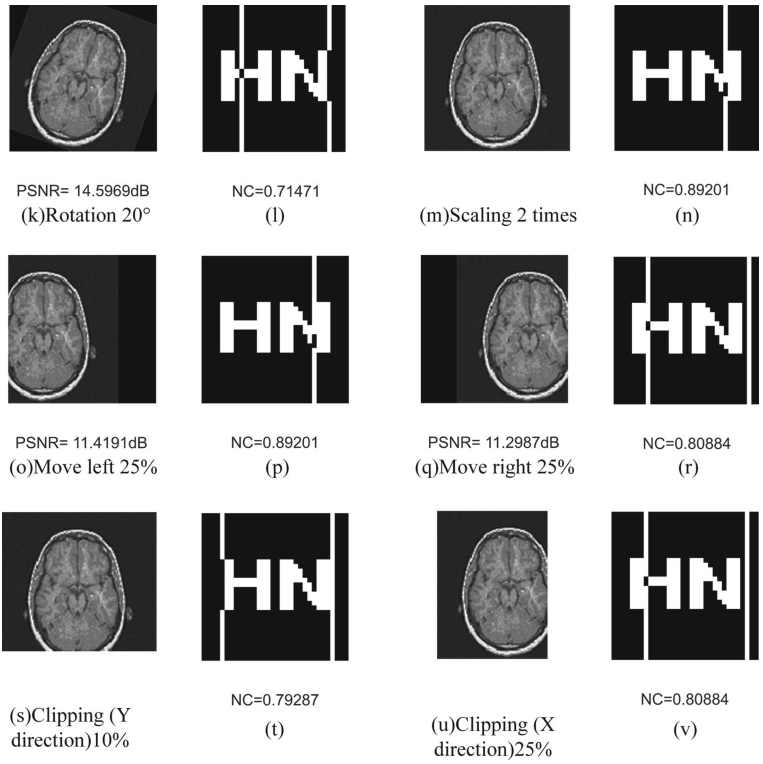

Fig. 8. Medical image and the restored watermark under geometric attacks.

(4) Crop attacks: As it can be seen in Table 3, compared with the ability to resist X-axis crop, the anti Y-axis crop ability of this algorithm is worse, but the NC value is still greater than 0.50 when the Y-axis is 25% cropped, and the NC value is as high as 0.81 when the X-axis is 25% which indicates that the algorithm has a good anti crop ability. In Fig. 8, (s) and (t) are the watermarks cut by 10% and restored by Y-axis, (u) and (v) are the watermarks cut by 25% and restored by X-axis respectively.

Combined with Table 3 and Fig. 8, it can be seen that the algorithm in this paper has a good ability to resist geometric attacks.

4.3 Algorithm Comparison

This paper compared the DCT algorithm and the Gabor-DCT algorithm. It can be seen from Table 4 that under common attacks, the watermark restoration effect of the DCT algorithm and Gabor-DCT algorithm is similar, and the NC value is close. However, under geometric attacks, the anti-rotation, translation, and crop of the Gabor-DCT algorithm are performing better than the DCT algorithm. Hence the Gabor-DCT algorithm is better than DCT in the anti-geometric attacks.

Table 4. Comparison of different algorithms.

	Attack	PSNR/dB		NC	
		DCT	Gabor-DCT	DCT	Gabor-DCT
Conventional attack	Gaussian noise 10%	11.85	11.85	0.78	0.74
	JPEG compression 1%	26.28	26.28	1.00	1.00
	Median filter 7×7 (Thirty times)	24.96	24.96	1.00	0.90
Geometric attacks	Rotation 20° (clockwise)	14.60	14.60	0.51	0.71
	Scaling 2 times	/	/	1.00	0.89
	Translation 20% (left)	12.07	12.07	0.33	1.00
	Translation 25% (right)	11.30	11.30	−0.08	0.81
	Clipping 25% (Y direction)	/	/	0.63	0.61
	Clipping 25% (X direction)	/	/	−0.21	0.81

5 Conclusion

In this paper, Gabor texture feature extraction is combined with DCT algorithm to obtain a Gabor-DCT based zero watermarking algorithm for medical images. The algorithm extracted texture information of different scales and directions through Gabor transform, and used the "energy concentration" feature of the DCT algorithm to concentrate the extracted texture information. Then applied the extracted medical image features to associate with the watermark, and combined the cryptographic ideas to design the watermark algorithm. Experimental results show that the algorithm has strong robustness to both common attacks and geometric attacks, and can effectively protect the security of medical image information.

References

1. Brar, A.S., Kaur, M., Kaur, S.: Medical Image Watermarking. Lap Lambert Academic Publishing, Sunnyvale (2012)
2. Chen, J.Y., Tao, L.: An efficient image watermarking scheme based on Gabor transform. Guangdianzi Jiguang/J. Optoelectron. Laser **16**(11), 1363–1367 (2005)
3. Lee, C.-J., Wang, S.-D.: Fingerprint feature extraction using Gabor filters. Electron. Lett. **35**(4), 288–290 (1999)
4. Eswaraiah, R., Sreenivasa Reddy, E.: Medical image watermarking technique for accurate tamper detection in ROI and exact recovery of ROI. Int. J. Telemed. Appl. **2014**, 984646 (2014)
5. Jian-Hu, M.A., Jia-Xing, H.E.: A wavelet-based method of zero-watermark. J. Image Graph. (2007)
6. Kavadia, C., Lodha, A.: A review on spatial and transform domain digital watermarking techniques. Int. J. Adv. Res. Comput. Sci. **04**(08), 20–22 (2013)
7. Kundur, D., Hatzinakos, D.: Digital watermarking using multiresolution wavelet decomposition. In: Proceedings of the 1998 IEEE International Conference on Acoustics, Speech and Signal Processing, ICASSP 1998 (Cat. No.98CH36181), vol. 5, pp. 2969–2972 (1998)

8. Liu, J., He, X.: A review study on digital watermarking. In: International Conference on Information and Communication Technologies (2006)
9. Lyons, M., Akamatsu, S., Kamachi, M., Gyoba, J.: Coding facial expressions with Gabor wavelets. In: Proceedings Third IEEE International Conference on Automatic Face and Gesture Recognition, pp. 200–205 (1998)
10. Nyeem, H., Boles, W., Boyd, C.: A review of medical image watermarking requirements for teleradiology. J. Digit. Imaging **26**(2), 326–343 (2013). https://doi.org/10.1007/s10278-012-9527-x
11. Perlman, R., Kaufman, C., Speciner, M.: Network security: private communication in a public world. Pearson Education India (2016)
12. Singh, S., Singh, R., Singh, A.K., Siddiqui, T.J.: SVD-DCT based medical image watermarking in NSCT domain. In: Hassanien, A.E., Elhoseny, M., Kacprzyk, J. (eds.) Quantum Computing: An Environment for Intelligent Large Scale Real Application. SBD, vol. 33, pp. 467–488. Springer, Cham (2018). https://doi.org/10.1007/978-3-319-63639-9_20
13. van Schyndel, R.G., Tirkel, A.Z., Osborne, C.F.: A digital watermark. In: Proceedings of 1st International Conference on Image Processing, vol. 2, pp. 86–90 (1994)
14. Williams, P.A.: Medical data security: are you informed or afraid? Int. J. Inf. Comput. Secur. **1**(4), 414–429 (2007)
15. Xiao, M., Wan, X., Gan, C., Du, B.: A robust DCT domain watermarking algorithm based on chaos system. Proc. SpIE **7495**, 183 (2009)
16. Yaxun Zhou, Wei Jin: A novel image zero-watermarking scheme based on DWT-SVD. In: 2011 International Conference on Multimedia Technology, pp. 2873–2876 (2011)
17. Zhuang, J.Z.: Digital watermarking technology. Computer Knowledge and Technology (2009)